Permanent Magnet DC Motor Brush Transient Thermal Analysis

Jacek Junak[1], Grzegorz Ombach[1], Dave Staton[2]
1 – VDO Automotive AG, Werner-von-Siemens 3, D-97076, Wuerzburg, Germany
2 – Motor Design Ltd. 1 Scotland Street, Ellemere, Shropshire, SY12 OEG, UK,
jacek.junak@continental-corporation.com, grzegorz.ombach@continental-corporation.com, dave.staton@motor-design.com

***Abstract* - Despite the increased use of brushless permanent magnet motors over past 25 years, the permanent magnet dc commutator motor (PMDC) is still widely used in automotive applications. This is due to their low cost and simple drive requirements. The prediction of the brush temperature is important for applications that do not have a constant load, but have short duration overloads. Such intermittent loads are typical in applications such as electron-hydraulic systems (e.g. anti-lock brake systems – ABS/EPS) and auxiliaries such as windscreen wipers. This paper gives details of an analytical thermal model developed for the prediction of thermal transients in PMDC motors and in particular the brushes. This is important for lifetime expectancy analysis of the motor**

I. INTRODUCTION

Permanent magnet dc commutator (PMDC) motors are still widely used in low cost automotive applications. Some of the applications such as anti-lock (ABS/EPS) braking systems have intermittent loads with short duration high overloads. The motor must be able to withstand such transient loads without excessive temperature rise within the winding and brushes. Thermal analysis is important in such cases to fully understand the thermal behavior of the machine and how it is influenced by design options, which include the electromagnetic circuit optimization and winding insulation material selection. The thermal behavior of the machine is a key component in lifetime expectance analysis.

Details of the motors and thermal transient tests carried out to help develop an accurate thermal model for the PMDC motor are given in section II. The analytical thermal model developed to predict the temperature rise of the motor and in particular the thermal transient performance of the brushes and commtator is given in section III. Section IV compared the calculated thermal transient response of the brushes for two 13-slot motors with various measured transients. Section V compared the calculated thermal transient response of the winding, rotor, stator and commutator for two 7-slot motors, one having a Nomex slot liner and the other having a powder slot liner. The advantage of the powder liner in terms of heat transfer capability and its ability to allow an overload for a longer time period is reported. The testing on the two 7-slot machines was at zero speed to eliminate losses other than in the armature winding and resistive losses in the brushes.

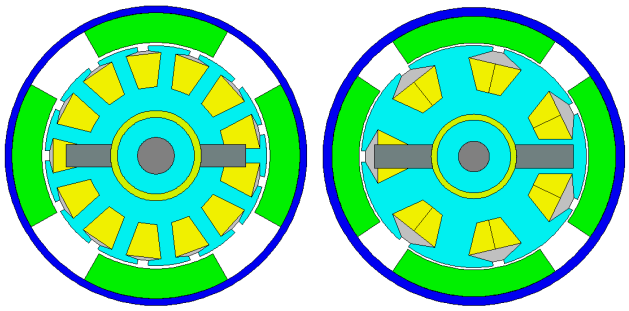

Fig. 1: Radial cross-section for the validation motors (Motors 1 and 2 on the left and Motor 3 on the right)

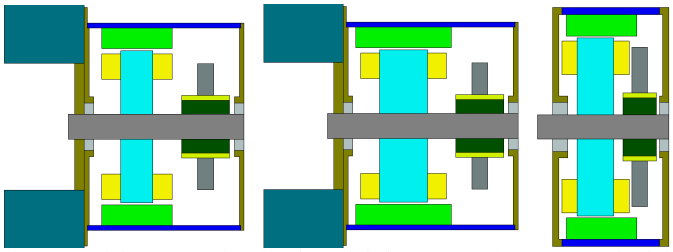

Fig. 2: Axial cross section for the validation motors (Motor 1 on the left, Motor 2 in the centre and Motor 3 on the right)

II. PMDC MOTORS USED FOR MODEL VALIDATION

Three sets of PMDC motors have been used for the validation of the thermal model. The radial and axial cross-sections for the machines are shown in Figs 1 and 2 respectively.

The first two motors have the same 13 slot, 4 pole radial cross-section, but have varying axial lengths, i.e. 10mm (Motor 1) and 15mm (Motor 2) armature lengths and 22mm and 30mm magnet lengths respectively. A relatively large magnet overhang is typical in low cost ferrite magnet motors to give an increase in flux/pole. The main dimensions for the first two motors are 66mm outer diameter, 1.5mm housing thickness, 6.5mm magnet thickness, 0.7mm air gap, 48mm rotor diameter, 3.25mm tooth width, 9.1mm slot depth, 2.3mm slot opening and 8mm shaft diameter. A picture of one of one the machines is shown in Fig 3. In the application it is mounted to a 100mmx100mmx25mm pump block. This is also shown in Fig 2 and 3. The pump block forms a large mass that must be accounted for in the thermal transient calculation. A picture of one of the brush card and the thermocouples attached to the

978-1-4244-1736-0/08/$25.00 ©2008 IEEE

brushes are shown in Fig 4. The short motor has a no-load speed of 6000rpm and a stall torque and current of 0.8Nm and 55A. The longer motor has a no-load speed of 6300rpm and a stall torque and current of 1.4Nm and 108A. The following transient tests were performed on the machines:

- Motor 1, 20A for 10 seconds, 5000rpm, 125C ambient
- Motor 2, 48A for 10 seconds, 5000rpm, 87C ambient
- Motor 2, 37A for 10 seconds, 5000rpm, 95C ambient
- Motor 1, 3 cycles of 20A for 7.5 seconds at 3000rpm followed by 30 seconds off, 100C ambient

The third motor has 7-slots. It has a 78mm outer diameter and 38mm axial length. Photographs of the rotor, commutator, housing and magnets together with the thermocouple attachments are shown in Fig 5. The winding in the machine is wound around a single tooth similar to that shown in Fig 6.b. Two prototypes were made, one with a 1mm thick Nomex slot liner and one with a 0.9mm thick powder liner. The thermal conductivity values for the two liners are 0.12W/m.K and 0.45W/m.K respectively. Thermal transient tests were performed on the two machines with 20A supplied to the locked rotor until the winding temperature reached 200°C with a 25° to 30°C ambient. The times to reach 200°C were 88 seconds for the Nomex liner machine and 245 seconds for the powder liner machine. This indicates that the powder machine has a larger overload capability due to the improved conduction heat transfer through the liner.

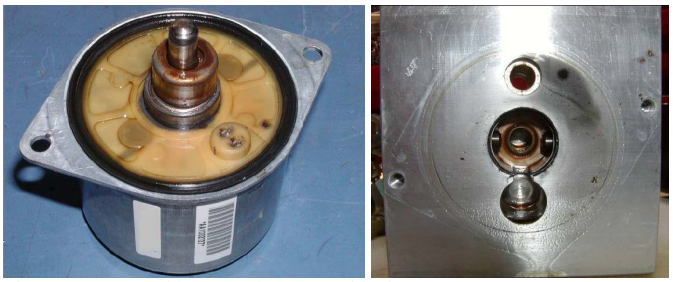

Fig. 3: Motor 1 and its mounting (pump block)

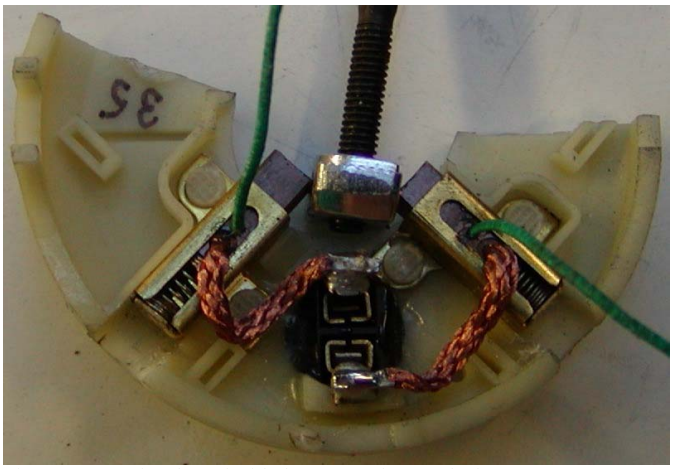

Fig. 4: Motor 1 brush card with thermocouples attached

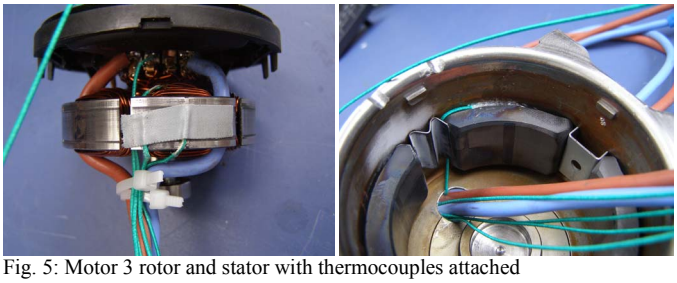

Fig. 5: Motor 3 rotor and stator with thermocouples attached

a) b)

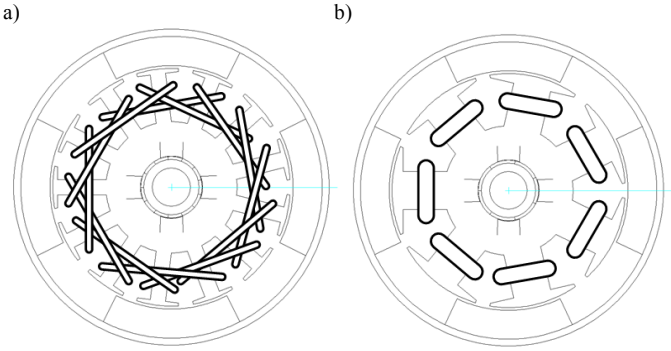

Fig. 6: Armature winding of calculated motors: a) Motors 1 and 2 (simplex wave winding); b) Motor 3 (single tooth winding)

III. Analytical Thermal Model for the PMDC Motors

The analytical thermal models presented here are implemented in the Motor-CAD software [1]. In the model, thermal resistances link important nodes within the motor cross-section and represent the main heat transfer paths. The nodes within the model are indicated on the radial and axial cross sections shown in Fig 7. The important nodes include the winding active copper, end-winding copper, armature tooth, armature back iron, armature surface, magnet surface, housing surface, commutator, brushes, etc.

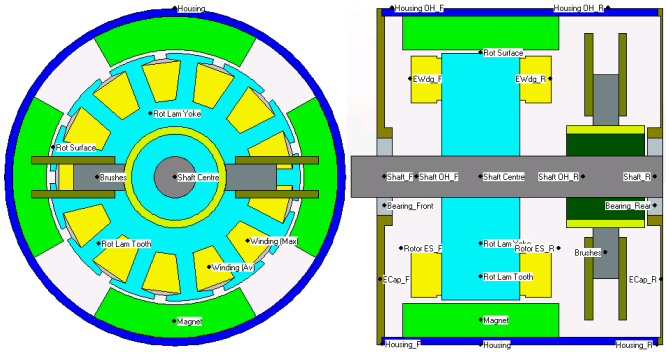

Fig. 7: Motor 2 radial and axial cross-sections showing the positions of nodes in the model (brush holders whose thermal capacitance are included in the model are also shown).

The conduction thermal resistances for the solid components are calculated from the components length (L), area (A) and thermal conductivity (k):

$$R = \frac{L}{kA} \quad (1)$$

Special mathematics have been developed to calculate the conduction thermal resistances of more complex composite components such as the winding where we have a mixture of copper, enamel, impregnation and air [2]. Equation (1) is also used to account for the interface resistance between components, with the effective interface gap estimated from research on typical gaps for different types of material [2] or by calibration with test data.

The convection and radiation thermal resistances for surfaces on the geometry are calculated from the surface area (A) and heat transfer coefficient (h):

$$R = \frac{1}{hA} \quad (2)$$

The heat transfer coefficient is a dissipation quantity and has units of W/m^2/C. The heat transfer coefficient for convection is calculated using well used and proven empirical convection correlations, many of which are available in heat transfer literature [2-7]. The radiation heat transfer coefficient is calculated using the formula:

$$h_R = \sigma \varepsilon F_{1-2} \frac{(T_1^4 - T_2^4)}{(T_1 - T_2)} \quad (3)$$

where σ = 5.669e-8 W/(m2K4), ε is the emissivity of the surface, F_{1-2} is the view factor for dissipating surface 1 to the absorbing surface 2 (the ambient temperature for external radiation) and T^1 and T^2 are the temperatures of surfaces 1 and 2 in units of Kelvin. The emissivity is a function of the surface material and finish for which data is given in most engineering text books [2-4]. The view factor can easily be calculated for simple geometric surfaces such as cylinders and flat plates, but it is a little more difficult for complex geometries, such as open fin channels. In these cases, books are available to help with the calculation of view factor [8,9].

Losses are added to the nodes at which they occur, i.e. copper loss in the winding, iron loss in the armature steel, brush loss in the brushes, etc. Thermal capacitances are added to the circuit to allow thermal transients to be calculated. A pictorial view of the thermal resistance network developed for a PMDC motor is shown in Fig 8.

As we are mainly interested in the temperature prediction of the brushes in this paper we will look at the thermal network in the region around the brushes and commutator in more detail. A diagram of this part of the network is shown in Fig 8. The model accounts for conduction heat transfer from the brush to the commutator, from the commutator to the shaft via the commutator insulation and from commutator to winding via the winding connections to the commutator. The conduction resistances are calculated using equation (1) together with the dimensions of the components and the thermal conductivity of the materials used. The convection from the brushes, brush holder and commutator is calculated using equation (2) with the surface area of the components calculated from the geometry and the heat transfer coefficient calculated using a special convection correlation developed with the aid of measurements within the endcaps of totally enclosed electric motors [2]. To development of an accurate but easy to use thermal model for the brushes and commutator is complicated due to the following issues:

- Heat transfer across the brush-commutator interface and brush friction loss both is a function of material properties, the brush spring force, wear, etc. In the model the user can provide an effective interface gap, with the contact area between the brush and commutator calculated from the brush and commutator geometry. An interface gap of 0.1mm is used in the models in this paper. More calibration research is required in the future to get a better estimate of typical gap for different brush materials and brush holders.
- The brush I2R loss is a function of the temperature due to the thermal resistivity of the brushes, This is taken account of in the simulation.
- The brush resistance varies with brush wear. Measurements can be made to help with calibration, however, the resistance measurement is difficult to make accurately as it is quite small.
- The brush connections and brush holder have an influence of the cooling of the brushes due to the interface gap between the brush and brush holder and the complex convection on the surface. The well used convection correlations developed for internal surfaces in totally enclosed machines are used in this case [2].
- The brush holder has some mass which adds to the thermal capacitance and slows down the temperature rise. It was found important to include the thermal capacitance and convection from the brush holders and brush connections in the model. The brush holders for Motors 1 and 2 are shown in Fig 4 and their inclusion in the model depicted in Fig 9. Further research will be done to investigate if we require more nodes in the model to distribute the thermal capacitance rather than concentrate it at a few nodes.
- The brush temperature is measured at one point on the brush which may not coincide with the node location in the model.
- The commutator is a complex geometric component in itself which is much simplified in the model.
- Loses in the coils undergoing commutation are more complex than for coils with pure dc current.
- The conduction heat transfer from the winding to the commutator is modeled by the number of connections of the know wire size. The wire connection length is estimated from the geometry in this case.

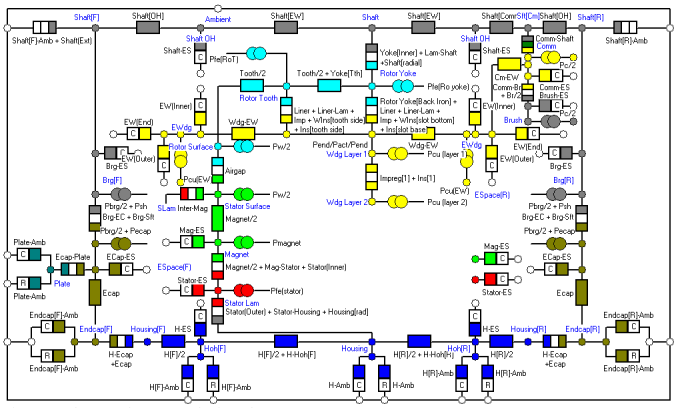

Fig. 8: Thermal network for the PMDC motor

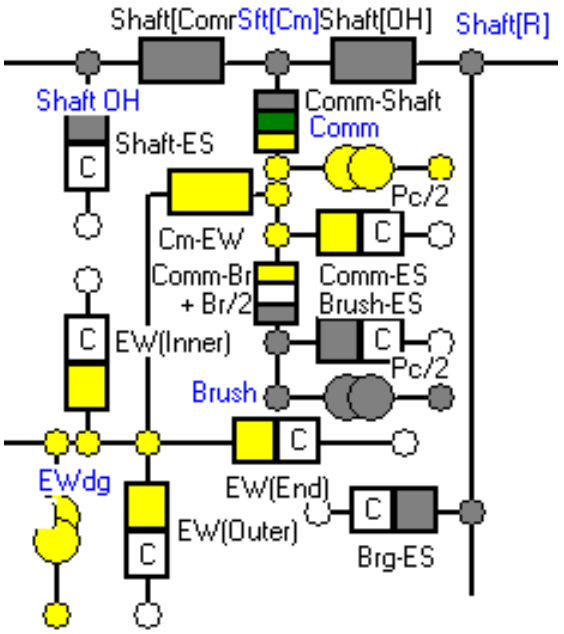

Fig. 9: Thermal network for the commutator and brushes

IV. Thermal Transient Results for the 13-Slot Motors

The transient tests detailed in section II were made on the two machines while installed on the test fixture shown in Fig 3. Comparisons between the measured and calculated thermal transients for the brushes are shown in Figs 10 to 13. It is seen that we get reasonable correlation between the measured and calculated results. It is seen that some of the calculations have a better match with measurements than others. This indicates that the cooling of the brushes and commutator is quite complex with some random effects occurring that are difficult to calibrate, i.e. the same model is used for both Motor 1 and Motor 2 with the same assumptions so it would be expected that the accuracy be similar for all tests. These difficulties were expected as some of the complexities listed in section III are difficult to calibrate for and can vary from machine to machine. This variation of heat transfer mechanisms from one machine to another is highlighted by the fact that the two brushes in the same machine can have a different thermal response as can be seen in Figs 10 to 13.

The transient duty cycle analysis shown in Fig 13 seems to be correctly predicting the heating sections of the characteristic but is over-predicting the cooling in off periods. More analysis is required to understand why this is the case, especially as in the cooling sections we have less unknowns as the losses are zero at this time.

Given all the complexities the brush and commutator model the accuracy of the prediction seems reasonable, especially as the model is just based on geometric dimensions with a few calibrated parameters such as the effective interface gap between brush and commutator and brush and brush holder. The model also only has a small number of nodes. Some simple sensitivity analysis has been done which indicates that the model is quite sensitive to the correct estimate of such quantities as the brush and brush holder thermal capacitance, brush loss, etc. Future research will be started soon carrying more detailed sensitivity analysis to get a full understanding of what is important in the model.

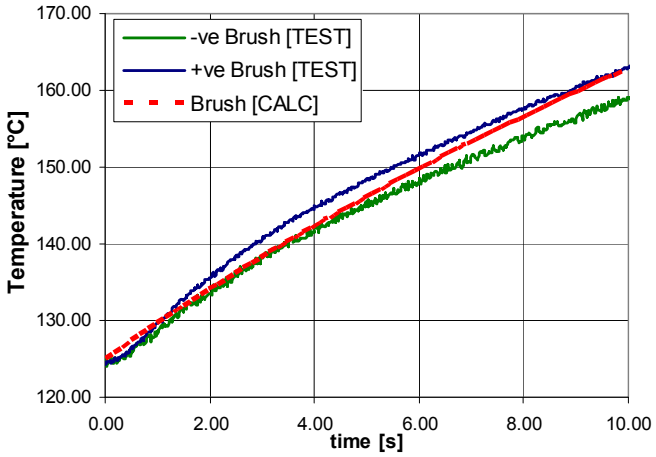

Fig. 10: Measured and calculated brush temperatures for the short Motor 1 (20A for 10 seconds).

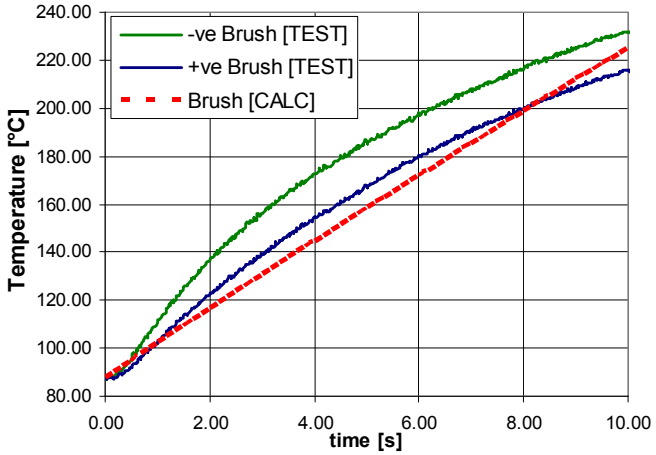

Fig. 11: Measured and calculated brush temperatures for the long Motor 2 (48A for 10 seconds).

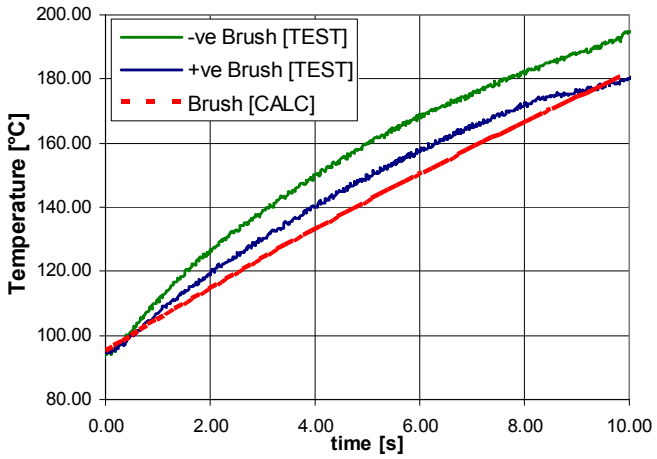

Fig. 12: Measured and calculated brush temperatures for the long Motor 2 (37A for 10 seconds).

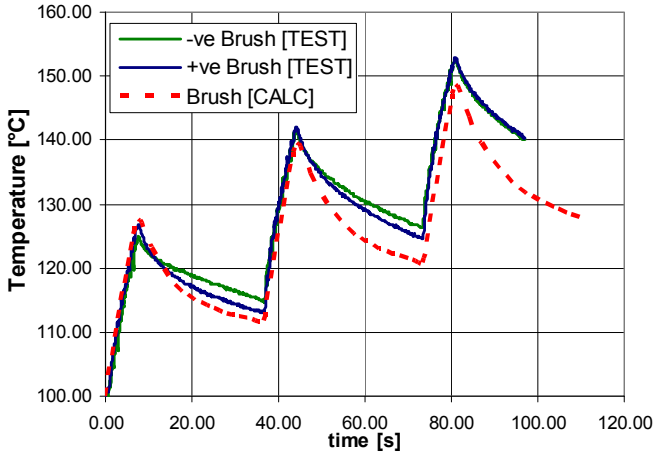

Fig. 13: Measured and calculated brush temperatures for the short Motor 1 (duty cycle of 20A for 7.5 seconds followed by 30 seconds off).

V. Thermal Transient Results for the 7-Slot Motor

The transient tests detailed in section II were made on two nearly identical 7-slot prototype motors. The only defference was that on motor has a 1mm thick Nomex slot liner and the other had a 0.9mm thick powder slot liner. Comparisons between the measured and calculated thermal transients for the winding, rotor, magnet, housing and commutator are shown in Figs 14 and 15. It is seen that we get reasonable correlation between the measured and calculated results. The heating of the winding is predicted very accurately but the cooling rate is under-predicted a little for some reason yet to be attained. The heating of the commutator is over-predicted somewhat but this could be due to the fact that we are predicting the average commutator temperature but in this case the motor is at zero speed and the coolest part of the commutator is measures at the furthest distance away from the brushes. A better result is expected when the motor is rotating. There are some small discrepancies between measured and calculated rotor, magnet and housing temperatures but the general form of the heating and cooling characteristics is predicted well. The discrepancies will be investigated further and reported in a later publication.

Fig 15 and 16 compare measures and calculated total loss for the two machines. The predictions accurately account for the added loss due to the temperature rise of the winding and brushes giving an increase in the winding and brush resistance. This is quite a large effect and must be accounted for in the calculation.

The advantage of the powder liner in terms of heat transfer capability and its ability to allow an overload for a longer time period is clearly shown in Figs 14 and 15. The times to reach 200°C were 88 seconds for the Nomex liner machine and 245 seconds for the powder liner machine. There is much better conduction heat transfer through the more highly conductive and slightly thinner powder liner than through the Nomex liner. The interface gap between the liner and armature lamination is also eliminated in the powder liner machine.

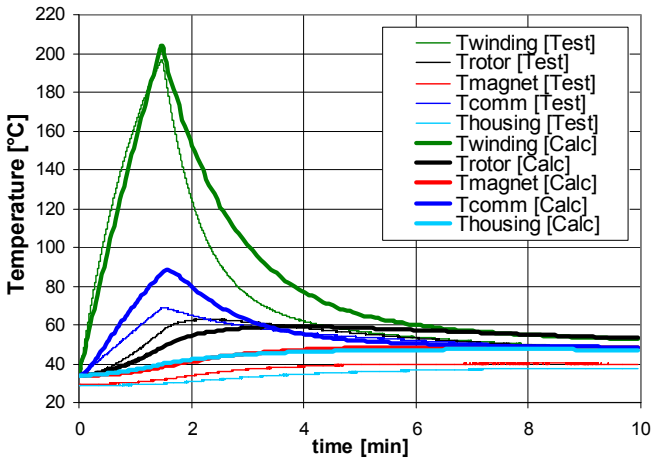

Fig. 14: Measured and calculated temperatures for Motor 3 with a Nomex liner (20A locked rotor until the winding reaches 200C then switched off)

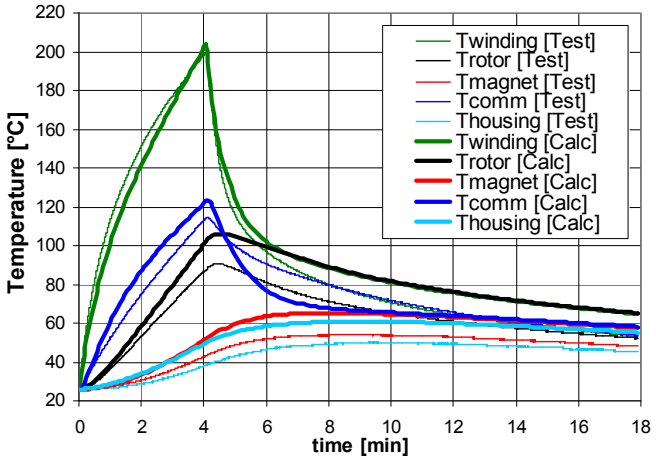

Fig. 15: Measured and calculated temperatures for Motor 3 with a Powder liner (20A locked rotor until the winding reaches 200C then switched off)

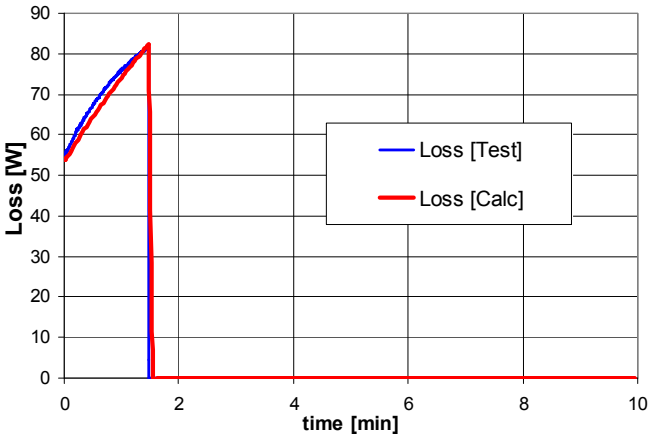

Fig. 16: Measured and calculated total motor loss for Motor 3 with a Nomex liner (20A locked rotor until the winding reaches 200C then switched off)

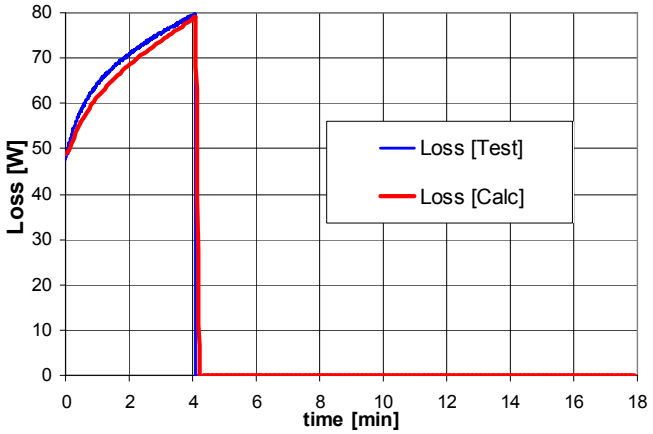

Fig. 17: Measured and calculated total motor loss for Motor 3 with a Powder liner (20A locked rotor until the winding reaches 200C then switched off)

VI. Conclusions

It has been shown that an analytical based thermal network model can be successfully used to calculate the thermal transient of the brushes in a PMDC motor. This can then be used to predict the temperature rise of the brushes with the various duty cycle types loads typically found in automotive applications. This is important in the analysis of motor life expectancy and for understanding what are the main design criteria to keep the brushes cool.

It has been demonstrated that a powder slot liner can give an improved overload capability compared to a Nomex liner.

The accuracy of the brush temperature calculation can be improved if certain key features in the model are calibrated, such as the brush resistance, brush friction loss and brush-commutator interface gap. More research for the future is proposed with the aim of improving the model accuracy and fully understanding the sensitivity of the model to design variables. Future research will be started soon carrying more detailed sensitivity analysis to get a full understanding of what is important in the model. Other future topics of research include; identifying the effective interface gap from brush to commutator and brush to brush holder; investigate the effect of brush material and brush holder design on the temperature response, development of improved convection and radiation models for the commutator, brush and brush holder surfaces.

Acknowledgment

Authors would like to thank VDO Automotive AG, Electric Motor Drives for support during preparation of that paper.

References

[1] Motor-CAD software manual, Motor Design Ltd, www.motor-design.com, UK

[2] D.A. Staton, A. Boglietti, A. Cavagnino, "Solving the More Difficult Aspects of Electric Motor Thermal Analysis, in small and medium size industrial induction motors", IEEE Transaction on Energy Conversion, Vol.20, n.3 pp.620-628.

[3] P.Mellor, D.Roberts, D. Turner, "Lumped parameter thermal model for electrical machines of TEFC design", IEE Procedings, Vol. 138, September 1991.

[4] F.P. Incropera, & D.P. DeWitt, D.P.: Introduction to Heat Transfer, Wiley, 1990

[5] J.P. Holman, Heat Transfer, McGraw-Hill, 1997, ISBN 0-07-844785-2

[6] A.F. Mills, Heat Transfer, Prentice Hall, 1999.

[7] A. Cavagnino, D. Staton, "Convection Heat Transfer and Flow Calculations Suitable for Analytical Modelling of Electric Machines", CD Conf. Rec. IECON06, 6-10 November 2006, Paris, France, pp. 4841-4846.

[8] S.N. Rea, S.E. West, "Thermal Radiation from Finned Heat Sinks", IEEE Transactions Hybrids, and Packaging, Volume 12, Issue 2, June 1976, pp. 115 – 117.

[9] M.F. Modest, Radiative Heat Transfer, Academic Press, 2003, ISBN 0125031637